

# Locomotion Performance of Amphibious Robot Vehicle using Transformable Rocker-bogie Mechanism

Zakariya Zainol<sup>1</sup>, Mohammed Rafeeq<sup>1</sup>, Siti Fauziah Toha<sup>1\*</sup> and Ahmad Syahrin Idris<sup>2</sup>

<sup>1</sup>Department of Mechatronics Engineering, Kulliyah of Engineering, International Islamic University, Malaysia.

<sup>2</sup>Department of Electrical and Electronics Engineering, University of Southampton Malaysia, Malaysia.

\*Corresponding author: tsfauziah@iium.edu.my, Tel: 6019-6035315.

**Abstract:** In the application of reconnaissance, post-disaster recovery, and search and rescue operations, researchers are significantly exploring amphibious robots owing to their excellent locomotion capabilities in diverse environments. An amphibious robot needs locomotion to maneuver on irregular, uneven terrains on land and a dynamic water medium. The study presents an amphibious robot that employs a rocker-bogie mechanism with an adjustable link providing retractable and unretractable configuration suitable on terrestrial and aquatic mediums. This paper proposes an amphibious robot vehicle (ARV) unretractable mode suitable for inclined locomotion on uneven land surface and retracted mode suitable for locomotion on water. Experiment investigation demonstrates Cross hill and downhill Grade ability on inclined surfaces that stabilize the ARV preventing it from slippage and flip over. The trainability and adaptability on land. The Simulation in Ansys for flow velocity vector shows retractable wheel position significantly improves trust forces by reducing the low bow losses. An integrated paddle mechanism will be employed in future design to increase the mobility on the Water Wheel.

**Keywords:** Locomotion, Retracted wheel, Rocker-bogie, Unretracted wheel

© 2021 Penerbit UTM Press. All rights reserved

*Article History: received 25 May 2021; accepted 12 June 2021; published 15 October 2021.*

## 1. INTRODUCTION

Amphibious robots research in the past two decades shows increasingly rising growth for a variety of applications. Recently, in reconnaissance, search and rescue operations, disaster relief utilizes amphibious robots for providing aid, equipment, repair, and recovery [1]. The arena post-disaster is chaotic, unstructured, and uneven to traverse to reach the target location. The locomotion in this area requires any mobile system's capability to pass through an obstacle, negotiate obstacles, ditches, traverse inclined paths, and various surfaces [2]. The challenging disaster area requires the vehicles to travel autonomously and perform the assigned task. The scenario involving a robot or autonomous vehicle to maneuver both land and shallow water requires the robot or autonomous vehicle to traverse unstructured land and water environments. There is a need for all-terrain vehicle ability on land and swimming capability on the water in a single system with compact control design.

Researchers studied amphibious robots in the last two decades because of their excellent locomotion capabilities in terrestrial and aquatic environments. Some of the works involve cockroach-inspired whogs series [3], basilisk lizard inspires to develop amphibious legged robot [4], wheeled amphibious ARGO [5], undulation locomotion of

salamander robot [6], Hybrid mechanism that relies on more than one mechanism for locomotion like eccentric mechanism [7], wheel leg propeller based amphibious robot [8]. However, the focus of the above-mentioned amphibious robots was on mobility in the aquatic medium. Also, they utilize a different mechanism for locomotion in a different environment.

To estimate the environment, researchers have used geometrical approaches [9], computer vision [10], and sensor-based [11] approaches for correctly mapping the environment. The real-time information from sensors or cameras is provided to the autonomous system to path plan or trajectory generation traversing through the surface. Tee et al. [12], The images obtained from aircraft or flying machines have lower details than obtained from the proximity of the disaster scene resulting in erroneous input to path planning. As discussed in [13], computer vision systems utilize a digital camera that provides real-time trajectory generation and navigation information. The information is suitable for amphibious robot operation. To reduce the risk for rescue personnel rescue mission employs autonomous agents to perform challenging mission tasks. The post-disaster rescue operations involve locomotion over irregular terrain profiles that involve obstacles of varying sizes, ditches, fallen trees, wetlands. The autonomous amphibious robot vehicle needs to

identify the target mission, mostly victim locomotion, and complete the operation efficiently, reducing risks [13].

Amphibious robots have similar design and performance as boats while sailing on the surface of the water. However, the amphibious robot vehicle design at the bottom poses more considerable water resistance than boats [14][15]. Mobile vehicle performance is studied using flow simulation analysis and experimentally validated with real-time data. Driving simulators are employed because of simplicity in operation, and training scenario performance is close to real time [16]. The driving simulators developed in the past are the University of Iowa created National Advanced Driving Simulator [17][18], Toyota Higashifuji Technical Center in Japan developed Toyota Driving simulator [19], provides amphibious robot vehicle performance analysis. Guixia et al. performed fluent simulation analysis to study the reduction of resistance by vehicle body when wheels are retracted, demonstrating significant resistance due to wheels position [16].

Amphibious robots on the terrestrial mode encounter various types of terrain profiles. The amphibious robot vehicle traverse over uneven terrains and slopes upward and downward [13]. The robot vehicle ought to have good trainability to pass over obstacles and uneven terrain profile. The trainability performance metric is improved by reducing wheel slip and maximizing traction of the robot vehicle. The performance metric on slopes is measure using the grade ability metric that provides vehicle ability to cross the inclined surfaces, and the torque requirement of the motor can be determined with the metric [20]. Zhu et al. uses downhill grade ability measure to minimize slip and cross hill grade ability to measures maximum angle of slope for a vehicle to cross on an inclined surface that prevents vehicle flip over [21].

ARV is built primarily for aid during pre-and post-disaster occurrences. The ARV was designed to have a characteristic of all-terrain vehicle and boat. The design concept of ARV was based on Amphibious All-Terrain Vehicle (AATV) [22]. The mechanical structure was enhanced by hybrid the rocker-bogie mechanism suspension to reduce the slip and chance to flip over during rough climbing terrain. The ARV uses integrated mechanism rocker-bogie passive suspension for adapting to different terrain profiles and a catamaran concept as a boat design for locomotion on water. The ARV hardware design is compact for traversing into the post-disastrous spaces that challenging and perilous. To inspect the disaster area and map the scene, ARV utilizes vision cameras mounted on the vehicle, powered by the battery. The functional controller with real-time information GPS as feedback to systems facilitates Navigation and Guidance. The ARV size is 0.7 meters long, 0.65-meter width, 0.24 meter high (retracted), and 0.35 meter in the land maneuver. The ARV weights 8 kg with dimensions (0.7 m in length, 0.65 m in width, 0.36 height m in Unretracted, and 0.24 m in height (retracted)). The ARV can traverse across diverse terrains on land and swimming in shallow water.

The study in this paper is organized as Section 1 introduces the work and previous literature study, the section presents the system integration and design capabilities of the system. In section 3, the simulation and analysis performed both on land and water, and the final

section highlights conclusions and future work.

## 2. SYSTEM INTEGRATION AND PROTOTYPE DESIGN

### 2.1 System Design Description

This system consists of a rocker-bogie mechanism, frame, off-road tire, and link retractable mechanism. The rocker-bogie mechanism allows the ARV to maneuver on uneven terrain and even capability to climbing over obstacles. The rocker-bogie mechanism avoids low oscillation frequency by distributing equal loads on all the wheels by averaging its pitch over all-wheel deflections.

The primary benefit of the mechanism is that the suspension requirement is evaded as the rocker-bogie distributes the load on all the wheels. It comprises a rocker connected to the frame and a bogie attached to the rocker link with the pivot joint. The author [13] uses a rocker-bogie mechanism to ensure even working conditions for all wheels and prevent excessive sinkage of a wheel in soft terrain (muddy). Figure 1 shows the mechanism of the ARV vehicle in retract condition, while Figure 2 shows the vehicle in the unretracted condition. Table 1 lists the ARV vehicle parameters for locomotion on land and water environment.

Table 1. Vehicle parameters

|                                   |                        |
|-----------------------------------|------------------------|
| Vehicle load                      | 8kg (78.4 N)           |
| Motor torque                      | 0.7848 Nm              |
| Tractive force on a single wheel  | 12.426 N               |
| Circumference of each wheel       | 0.377 m                |
| Coefficient of rolling resistance | 0.032 –<br>(Poor Road) |

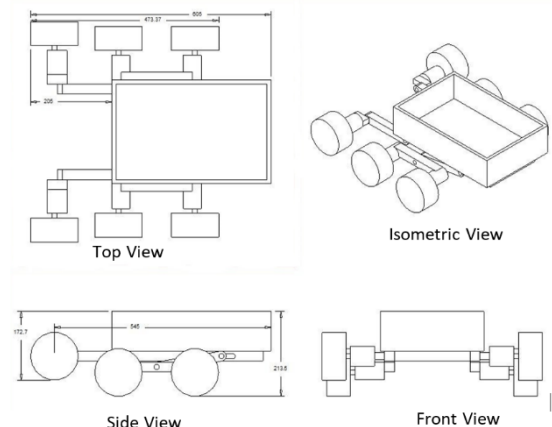


Figure 1. Chassis structure of ARV (retracted)

### 2.2 Gradeability Amphibious Robot on Inclined Surfaces

In the post-disaster scenario, for the robot vehicle to carry out the assigned task successfully, it is an important vehicle to get stuck, flip over, and slippage that risks the whole mission. To avoid such a scenario, grade ability analysis at the downhill, front, and cross hill provides significant input to stabilize the vehicle in static analysis

measurement of maximum inclined angle that stabilizes robot vehicle from flip over and slippage. Figure 3 illustrates parameters required in the measurement of downhill and front grade ability. The calculated value of downhill grade ability minimizes wheel slippage and maximizes vehicle traction. Flip over of robot vehicles at the slopes is prevented either by increasing vehicle width or tire radius. However, this changes overall vehicle specification and requires a different analysis.

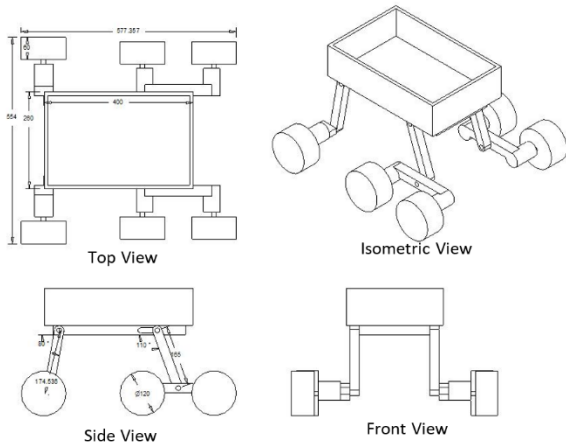


Figure 2. Chassis structure of ARV (unretracted)

To avoid such a scenario, grade ability analysis at the downhill, front, and cross hill provides significant input to stabilize the vehicle in static analysis measurement of maximum inclined angle that stabilizes robot vehicle from flip over and slippage. Figure 3 illustrates parameters required in the measurement of downhill and front grade ability. The calculated value of downhill grade ability minimizes wheel slippage and maximizes vehicle traction. Flip over of robot vehicles at the slopes is prevented either by increasing vehicle width or tire radius. However, this changes overall vehicle specification and requires a different analysis.

Cross hill measures the maximum angle the vehicle is required to cross over. The cross hill measurement is significant at post-disaster terrain maneuver as the scenario requires quick response without any fault that risks completing the task. P is the grade ability in percentage is calculated in Equation 1 as 91.8%,  $F_z$  is tractive force,  $G_z$  is overall combine mass and  $f_r$  rolling friction coefficient as in Table 1. The angle of the gradient in degree is calculated as in Equation 2 as 42.55°.

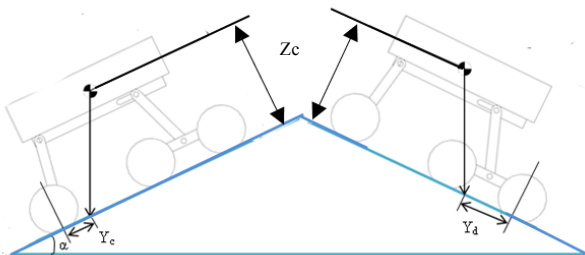


Figure 3. Downhill and Front grade ability

$$p = 100 \left[ \frac{F_z}{9.81G_z} - f_r \right] \quad (1)$$

$$\alpha = \tan^{-1} p/100 \quad (2)$$

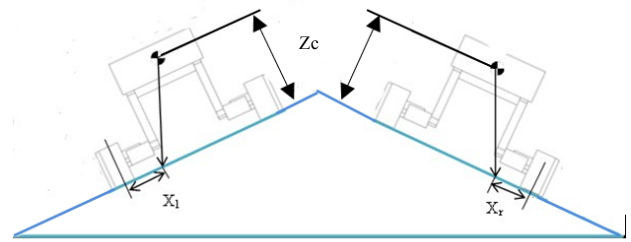


Figure 4. Cross hill grade ability

### 2.3 Hull Design and Floatability

Hull shape is vital to ARV speed and stability while water surface maneuvering cycle. The hull shape repels the water volume and makes it float on water. The stability requirement of vessels is imperative; therefore, the catamaran design concept is chosen to facilitate large spacing between hulls increasing stability maintaining fuel efficiency. Displacement-type catamarans have a round hull shape that adds to the stability of the vessel. Figure 5 shows the catamaran hull from the front view. The catamarans were designed from two hulls that connected each other. The catamaran design also provides a height ground clearance made it easy to pass high obstacles when in land mode. The retracted wheel is positioned inside the hull, as shown in Figure 6. To make ARV more stable on the water, one-third of the body should be submerged in the water. The submerged also give a wheel fully contact with water surface since the wheel act as water propulsion. The total volume required to make the ARV safely float from Equation 3 is 0.0136 m<sup>3</sup>.

$$Volume, V = \frac{SOPHIBIAN \text{ Mass, kg} \times \text{Safety Factor}}{\text{Fluid Density, kg/m}^3} \quad (3)$$

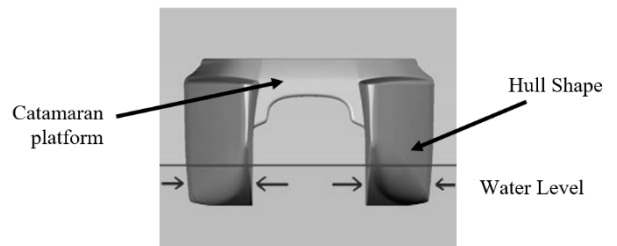


Figure 5. Catamaran Hull

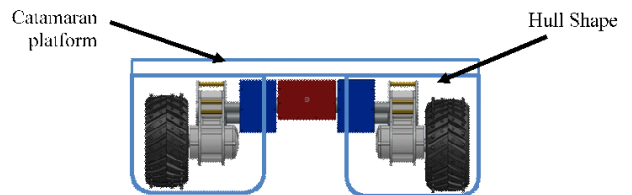


Figure 6. Mechanical structure of ARV in the catamaran.

## 3 RESULTS AND DISCUSSION

### 3.1 Locomotion Performance on ground

The highest grade a vehicle can ascend while maintaining a particular speed defines the grade ability. In the analysis of ascending slope, the vehicle locomotion is limited by

weight and angle of inclination of the road surface as in Equation 4 [20]. This paper focuses on the relation of the distance between the centers of a body towards the terrain surface. The vehicle operates in two modes, retracted and unretracted; servos adjust the rocker-bogie mechanism links to either of these modes by changing the angle  $\alpha_{max}$  it is calculated using Equation 4 and Equation 5. The ARV parameters from Figure 7 where  $L_{cd}$  is a distance from the vehicle's center of the front wheel, and  $L_{cc}$  is the vehicle's center distance towards the rear wheel. The  $z_c$  is a distance of the vehicle's center towards the ground surface, while  $b_c$  is a distance of wheel to the centre at the front view.

The downhill Gradeability angle is affected by  $L_{cc}$  and  $z_c$ , and the front-hill Gradeability angle by  $L_{cd}$  and  $z_c$  contribute. Whereas in the case of cross-hill Gradeability angle  $b_c$  is constant and is subjected only to changes of  $z_c$ . The vehicle stability increases by lowering the distance of the center of a vehicle to the ground. Therefore,  $Z_c$  is the critical parameter in the analysis. Figure 7 shown the variables link of vehicles.

$$\alpha_{max} = \min \left\{ \tan^{-1} \frac{Y_d}{z_c}, \tan^{-1} \frac{Y_c}{z_c} \right\} \quad (4)$$

Where  $y_c = \tan^{-1} \alpha$ , and  $Y_c = L_{cc} - Y$

The amphibious robot vehicle roll, pitch, and yaw angle output in both retracted and unretracted are affected by four input variables of vehicle  $L_{cc}$ ,  $L_{cd}$ ,  $z_c$ , and  $b_c$  as summarized in "Table 2". The roll angle output is affected by input  $z_c$  and  $b_c$  variables, and pitch angle output is affected by  $L_{cd}$ ,  $L_{cc}$ , and  $z_c$ . Thus, Table 3 states the angle of the vehicle in two different modes.

$$\alpha_{max} = \min \left\{ \tan^{-1} \frac{X_l}{z_c}, \tan^{-1} \frac{X_r}{z_c} \right\} \quad (5)$$

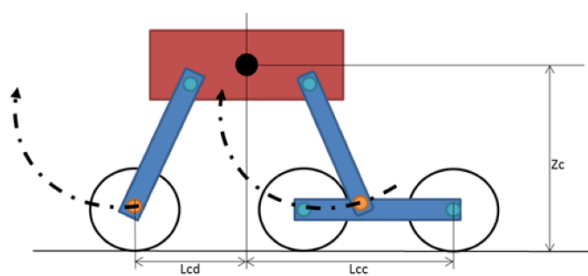


Figure 7. ARV vehicle variables

In the retracted mode in Table 4, the front hill grade ability and rear downhill grade ability is measured as 37°. The cross-hill grade ability maximum angle to cross is measured as 58°. In the unretracted mode, the front hill grade ability increases sharply to 69° putting load, increasing the motor torque requirement. However, rear downhill grade ability decreases to 31°, indicating a lower requirement of motor torque. The cross-hill grade ability maximum angle to cross is measured as 58°. In the overall system, the front hill grade ability ranges from 37° to 69° while the range 31° to 37° rear downhill grade ability is closer to the minimum angle requirement of 42.22°. The vehicle cross-hill grade ability measured ranges from 36° to 59°, making it suitable for the cross. Also, from Table 2 and Table 3 and based on Equation 4 and Equation 5,

pronounces the distance of the wheel toward the center mass continuously affects the angle of inclination of ARV.

Consequently, the results indicate the ARV is suitable for locomotion in the post-disastrous area (debris and covered mud damage most of the road surfaces) with an assumption of the poor road (low coefficient of friction). ARV can maneuver smoothly on inclined surfaces with an inclination angle of 42.55° using the minimum input motor torque of 0.7848 N on each wheel. The motor torque can be increased to optimize the incline angle achieved from a retractable wheel.

Table 2. Tyre distance form vehicle's centre

| Condition | Retract (cm) | Unretracted(cm) |
|-----------|--------------|-----------------|
| Zc        | 265          | 120             |
| bc        | 195          | 195             |
| Lcc       | 200          | 315             |
| Lcd       | 200          | 73              |

Table 3. Angle of vehicle for two difference condition

| Grade ability                | Retract(°) | Unretracted(°) |
|------------------------------|------------|----------------|
| Front Hill (Pitch)           | 37         | 69             |
| Rear Downhill (Pitch)        | 37         | 31             |
| Left-Right Cross hill (Roll) | 36         | 58             |

### 3.2 Locomotion performance on the water

The simulation is performed using the Ansys platform to reduce the bow wave loss at the vehicle wheel position. The simulation involves the mechanism mode in retracted and unretracted wheel positions. The analysis assumes water current in steady-state and setting the flow velocity at 10 m/s. The vehicle chassis is positioned at the interface of water and air medium. The servos control wheel rocker and bogie links are appended to chassis in retracted or unretracted modes.

In the unretracted mode, position the wheels under the surface of the robot body as in Figure 8 demonstrates blocks and disturb the water flow in the direction of water flow. The distraction of water at wheels creates high pressure before (front end) the wheel marked as region 1 and low pressures after (rear end) the wheel marked as region 2. This unequal distribution results in the creation of negative pressure affecting both the stability and thrust of the vehicle. Also, the low pressure creates a whirlpool flow between the wheels, increasing bow wave losses. The whirlpool occurs between wheel 1 and wheel 2, and wheel 2 and wheel 3 are due to opposing currents in the region between the wheels. The whirlpool further creates a surface current to change direction due to rapid swirl spiraling waves. This effect reduces the overall loss of vehicle speed. Figure 8 illustrates the velocity vector with region 1 velocity at 6.1626 m/s and region 2 velocity at

3.1126 m/s. This difference in velocity at the front and rear end of the wheel develops a behavior increasing the drag force of the vehicle. The required force to maneuver increases because of increased bow loss and pressure difference at the wheel.

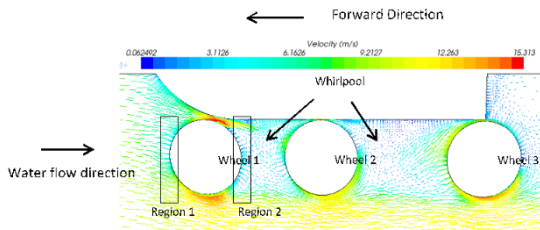


Figure 8. Unretract Wheel-deployed (Velocity Vector)

The simulation of the vehicle in a retracted mode in Figure 9 demonstrates the flow across the wheels. The wheel is aligned near the vehicle's chassis in the retracted position, leaving a shallow space between the vehicle under the surface and the wheels. The velocity vector under a vehicle is smooth in a single direction without any distractions. The minimal pressure difference is between the wheels in a retracted position eliminates the whirlpool created during the unretracted mode. The drag force for the vehicle reduces because of minimal whirlpool allowing the vehicle to maneuver with its actual force and velocity. However, the hull rear retracted wheel position produces a circular wave pattern, reducing the flow velocity.

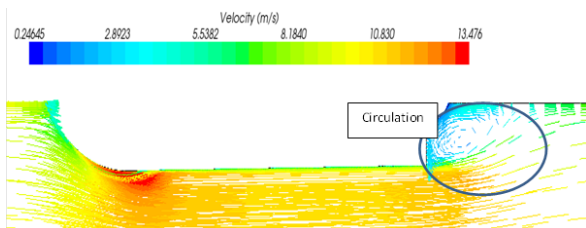


Figure 9. Retract Wheel-deployed (Velocity Vector)

#### 4. CONCLUSION

The article presents a novel amphibious robot that has versatile locomotion competence both on land and the water environment. The amphibious robot employs a rocker-bogie mechanism as a passive suspension mechanism connected to six wheels using rocker and bogie links. The simulation and the experimental study confirm that robots in unretracted mode are suitable for locomotion on land with higher mobility and adaptable to uneven terrain profiles. However, the mobility performance on water is better in the retracted mode of the ARV. The downhill and cross hill grade ability tests inclined motion for ARV; the grade ability metric measures stability and preventing the ARV from flipping over and slippage during the cross. The advantages of the final design are linear locomotion, stability in climbing either front uphill or rear downhill. The intelligent control capability will further enhance the traction on-ground locomotion, and mobility performance on water using wheelpaddle mechanism is under future work.

#### ACKNOWLEDGMENT

The author would like to acknowledge financial assistance from the Malaysia ministry of education under the FRGS Grant FRGS17-031-10597. We would like to thank the financial support of IIUM under the KOE postgraduate Tuition fee waiver scheme 2019 (TWF2019).

#### REFERENCES

- [1] B. Zhong, Y. Zhou, X. Li, M. Xu, and S. Zhang, "Locomotion Performance of the Amphibious Robot on Various Terrains and Underwater with Flexible Flipper Legs," *J. Bionic Eng.*, vol. 13, no. 4, pp. 525–536, Oct. 2016.
- [2] M. Rafeeq, S. F. Toha, S. Ahmad, and M. A. Razib, "Locomotion Strategies for Amphibious Robots-A Review," *IEEE Access*, vol. 9, pp. 26323–26342, 2021.
- [3] R. Harkins, J. Ward, R. Vaidyanathan, A. S. Boxerbaum, and R. D. Quinn, "Design of an autonomous amphibious robot for surf zone operations: Part II - Hardware, control implementation and simulation," in *IEEE/ASME International Conference on Advanced Intelligent Mechatronics, AIM*, 2005, vol. 2, pp. 1465–1470.
- [4] S. Floyd, T. Keegan, J. Palmisano, and M. Sitti, "A novel water running robot inspired by basilisk lizards," in *IEEE International Conference on Intelligent Robots and Systems*, 2006, pp. 5430–5436.
- [5] S. Khaled, "Speed Control of Autonomous Amphibious Vehicles," 2017.
- [6] X. Yin, C. Wang, and G. Xie, "A salamander-like amphibious robot: System and control design," *2012 IEEE Int. Conf. Mechatronics Autom. ICMA 2012*, pp. 956–961, 2012.
- [7] Y. Sun and S. Ma, "ePaddle mechanism: Towards the development of a versatile amphibious locomotion mechanism," in *IEEE International Conference on Intelligent Robots and Systems*, 2011, pp. 5035–5040.
- [8] Y. Tang, C. Liu, A. Zhang, and J. Yu, "Optimal distribution of propulsion for an amphibious robot based on wheel-propeller-leg mixed thrusters," *11th Int. Conf. Control. Autom. Robot. Vision, ICARCV 2010*, no. December, pp. 822–826, 2010.
- [9] D. Filliat and J. A. Meyer, "Map-based navigation in mobile robots: I. A review of localization strategies," *Cogn. Syst. Res.*, vol. 4, no. 4, pp. 243–282, 2003.
- [10] Z. Chen, J. Samarabandu, and R. Rodrigo, "Recent Advances in Simultaneous Localization and Mapping (SLAM) for Mobile Robots," *Adv. Robot.*, vol. 21, no. 4, pp. 233–265, 2007.
- [11] J. Jeong, T. S. Yoon, and J. B. Park, "Multimodal sensor-based semantic 3D mapping for a large-scale environment," *Expert Syst. Appl.*, vol. 105, pp. 1–10, 2018.
- [12] Y. H. Tee, Y. C. Tan, B. Y. Teoh, E. B. Tan, and Z. Y. Wong, "A compact design of zero-radius steering autonomous amphibious vehicle with direct differential directional drive - UTAR-AAV," *2010 IEEE Conf. Robot. Autom. Mechatronics, RAM 2010*,

- pp. 176–181, 2010.
- [13] M. Frejek and S. Nokleby, “Design of a Small-Scale Autonomous Amphibious Vehicle,” in *2008 Canadian Conference on Electrical and Computer Engineering*, 2008, pp. 781–786.
  - [14] S. Guixia and Z. Youqun, “The design of wheel retraction function of the amphibious vehicle,” *2008 IEEE Veh. Power Propuls. Conf. VPPC 2008*, pp. 8–11, 2008.
  - [15] W. Tao, Q. Guo, and G. Xu, “Simulation for Flow Field around Sailing Amphibious Vehicle,” *J. Syst. Simul.*, vol. 19, no. 22, pp. 5130–5153, 2007.
  - [16] S. Zheng, Z. Ye, Z. Yang, and J. Han, “The special amphibious vehicle driving simulator design and development,” *2012 Spring World Congr. Eng. Technol. SCET 2012 - Proc.*, pp. 8–11, 2012.
  - [17] L. Chen and Y. Papelis, “NADS at the University of IOWA: A tool for driving safety research,” *Proc. 1st ...*, vol. 2001, pp. 1–14, 2001.
  - [18] G. J. Heydinger, M. K. Salaani, W. R. Garrott, and P. A. Grygier, “Vehicle dynamics modelling for the National Advanced Driving Simulator,” *Proc. Inst. Mech. Eng. Part D J. Automob. Eng.*, vol. 216, no. 4, pp. 307–318, 2002.
  - [19] P. McNamara, “Inside Toyota’s \$15m driving simulator, [http:// www.car magazine.co.uk//Car-Magazine-Blogs/Phil-McNamara-Blog/Inside-Toyota-15m-driving-simulator/](http://www.car-magazine.co.uk/Car-Magazine-Blogs/Phil-McNamara-Blog/Inside-Toyota-15m-driving-simulator/),” *2009, Nov.* .
  - [20] A. Yamsani, “Gradeability for Automobiles,” in *IOSR Journal of Mechanical and Civil Engineering (IOSR-JMCE)*, vol. 11, no. 2, pp. 35–41.
  - [21] J. Zhu, Y. Wang, H. Yu, W. Wang, and Y. Wen, “Sensing incline terrain for mobile robot autonomous navigation under unknown environment,” *2010 IEEE Int. Conf. Inf. Autom. ICI A 2010*, vol. 1, no. 1, pp. 2296–2301, 2010.
  - [22] J. B. Coast, “Tracked, amphibious vehicle with track securement and guide means.” US Patent 4,433,634, 1984.